minerals

MDPI

Article

Study on Chalcopyrite Dissolution Mechanism and Bioleaching Community Behavior Based on Pulp Concentration Gradient at 6 °C

Xiao Jiang [1,2], Meilian Man [1,2] and Weimin Zeng [1,2,*]

[1] School of Minerals Processing and Bioengineering, Central South University, Changsha 410083, China; 215611011@csu.edu.cn (X.J.); manmeilian@csu.edu.cn (M.M.)
[2] Key Laboratory of Biometallurgy, Ministry of Education, Changsha 410083, China
* Correspondence: zengweimin1024@126.com

Abstract: Low-temperature bioleaching is relevant to the recovery of metals in alpine mines, but its development has been constrained by low bioleaching rates at high pulp concentrations. To this end, the bioleaching effect of the microbial community after the domestication of pulp concentration at 6 °C was studied. Domestication improved the bioleaching rate of copper. Environmental scanning electron microscopy (ESEM), X-ray diffraction (XRD), and electrochemical measurements revealed that the domestication process aggravated the corrosion of the chalcopyrite surface by accelerating its dissolution reaction. High-throughput sequencing technology indicated that *Acidithiobacillus* spp., *Leptospirillum* spp., and *Acidiphilium* spp. were the major lineages of the domesticated microbial community. The analysis of the microbial community revealed that domestication changed the microbial structure, enhancing the adaptability of the microbial community to pulp concentrations and acidic conditions. This study uncovered the mechanism by which domestication enhanced the bioleaching efficiency of the microbial community at low temperatures.

Keywords: chalcopyrite; low temperature; domestication; microbial community action mechanism

check for updates

Citation: Jiang, X.; Man, M.; Zeng, W. Study on Chalcopyrite Dissolution Mechanism and Bioleaching Community Behavior Based on Pulp Concentration Gradient at 6 °C. *Minerals* **2024**, *14*, 698. https://doi.org/10.3390/min14070698

Academic Editor: Jean-François Blais

Received: 31 May 2024
Revised: 28 June 2024
Accepted: 3 July 2024
Published: 8 July 2024

Copyright: © 2024 by the authors. Licensee MDPI, Basel, Switzerland. This article is an open access article distributed under the terms and conditions of the Creative Commons Attribution (CC BY) license (https://creativecommons.org/licenses/by/4.0/).

1. Introduction

Chalcopyrite is the most abundant copper-bearing resource in the world [1]. Traditional pyrometallurgical technology is a method to effectively process sulfide ores, but it is restricted by the high consumption of resources and the serious pollution of the ecological environment. Bioleaching, as a environmentally friendly method, offers a superior alternative for treating low-grade sulfide ores [2]. This method is highly efficient and cost-effective in extracting metals from sulfide ores, particularly for certain types of ores like low-grade ores, tailings, and waste ores that traditional techniques fail to process economically and efficiently. With the increasing implementation of environmental protection policies [3] and the explosive growth in demand for mineral resources, it becomes increasingly crucial to fully leverage the unique benefits of bioleaching.

Current research on the bioleaching of sulfide minerals is mainly carried out under regular or high temperatures, while studies at low temperatures (<10 °C) are scarce. However, some studies have been performed below 10 °C. These studies have found that specific microorganisms could catalyze the dissolution minerals [4–6]. Langdahl and Ingvorsen found that minerals sourced from northern Greenland could reach 30% of the maximal value of mediated dissolution [7]. It was discovered that *Acidithiobacillus ferrivorans* SS3 could leach pyrite at 4 °C [8]. Tangjian Peng et al. reported that *Acidithiobacillus ferrivorans* YL15 extracted copper (1.92 g/L) from chalcopyrite at 6 °C [9]. Low-temperature bioleaching can broaden the scope of bioleaching, which is particularly vital for initiating and maintaining bio-heap bioleaching operations in some areas such as those at high latitudes and altitudes.

Although low-temperature bioleaching technology holds vast potential for diverse applications, it encounters numerous challenges, particularly when dealing with high pulp concentrations. The limited adaptability of microorganisms under such conditions often results in reduced bioleaching efficiency and metal recovery. Several studies have proven that bioleaching efficiency can be enhanced through ore pretreatment [10], the addition of co-bioleaching agents [11], and the elimination of passivation films [12]. However, there is scarcely any research on strategies for adapting microorganisms to high pulp concentrations. Recent investigations indicated that pulp concentration significantly influences bioleaching kinetics, and that the judicious modulation of this parameter could optimize the bioleaching process, thereby augmenting the bioleaching rate [13–15]. These findings provided robust support for further mechanistic studies on pulp concentration acclimatization.

The process of extracting metals from sulfide ores through bioleaching is fundamentally an electrochemical reaction involving oxidation. Studies using electrochemical methods such as cyclic voltammetry (CV) have revealed that sulfide minerals, including chalcopyrite, form intermediates and exhibit specific electrochemical signals during dissolution. The efficiency of this dissolution is influenced by corrosion potential and corrosion current [16–18]. The analysis of the microbial community is frequently applied to research on bioleaching processes of sulfide minerals. It has been demonstrated that the metal extraction rate is higher when using a microbial community for bioleaching than when using monobacterial cultures [19–21]. Species such as *Acidithiobacillus* spp., *Leptospirillum* spp., *Sulfobacillus* spp., and *Ferroplasma* spp. could commonly be identified in bioleaching operations at moderate and/or medium–high temperatures where they played diverse roles including iron or sulfur oxidation and the utilization of inorganic or organic substances [22–26]. The synergy among *Acidithiobacillus ferrianus*, *Sulfobacillus thermotolerans* and *Metallosphaera sedula* could increase the efficiency of ferrous iron oxidation [27]. In contrast, there were few studies on bioleaching using a microbial community at low temperatures. Halinen et al. reported the initial occurrence of various *Acidithiobacillus* species, followed by the discovery of *At. ferrooxidans*, and *Ferromicrobium*, *Acidophilum*-affiliated organisms, and Gram-positive bacteria after a 500-day period [28]. Zepeda et al. found that the mixed microflora was able to leach low-grade copper sulfide ore at 10 °C with a certain bioleaching effect [29].

Mines in cryogenic regions are widely distributed worldwide [30,31]. Cryogenic biometallurgy is favorable to the metal recovery of these mines. The low-temperature biometallurgical process suffers from various difficulties, including a slow bioleaching rate and a low bioleaching rate. So it is crucial to enhance the metal bioleaching rate of low-temperature bioleaching. The aim of this study is to investigate the influence of pulp concentration domestication on the bioleaching efficiency under low-temperature conditions. The research methodology involved comparing the differences in bioleaching parameters before and after domestication. Additionally, the electrochemical behavior of chalcopyrite dissolution was characterized through cyclic voltammograms and potentiodynamic polarization diagrams. The morphological characteristics and material composition of minerals before and after domestication were characterized by environmental scanning electron microscopy (ESEM) and X-ray diffraction (XRD). Finally, the microflora composition and structure were measured using high-throughput sequencing. The findings of this study will contribute to the application of domestication in cryobiometallurgy and provide a theoretical foundation for the application of cryobiometallurgical technologies in the exploitation of low-temperature mines.

2. Materials and Methods

2.1. Microorganisms and Mineral

The higher purity chalcopyrite sample was obtained from Guangzhou City, Guangdong Province, China. The concentrate sample was mainly composed of chalcopyrite. According to XRD analysis, the sample was of high purity, and the main chemical elements were Cu (31.42%), Fe (31.99%), and S (36.58%). The chalcopyrite was crushed and passed through a sieve to achieve a granularity no larger than 75 μm, and subsequently subjected to ultraviolet sterilization for a full day within a sterile environment. The microbial consortium employed in this research was sourced through enrichment from the acidic drainage of Duobaoshan copper mine. For the collection of water samples, two locations within the Duobaoshan copper mine area were selected (an acidic tailing pool and a tailing dump). All samples were combined and then cultivated in iron-free 9K medium using chalcopyrite (1% pulp density) as a sole energy source at 6 °C The obtained mixed bacterial consortium was considered as the original community.

2.2. Bioleaching Experiments

The bioleaching of chalcopyrite was conducted based on pulp concentration gradient in 250 mL shake flasks. Experimental groups were, respectively, named D1, D2, and D3 according to the pulp densities of 1%, 2%, and 3%, while the control group was named Control. The flasks in all experiments were operated at 160 rpm and 6 °C. The bioleaching experiment conditions were as follows: the initial inoculation cell density was 2×10^7 cells/mL; the initial pH was 2.0; and the leaching period was 60 days. All bioleaching experiments were carried out in triplicate. The mixture derived from the aforementioned experiment underwent centrifugation at 2000× *g* to allow the ore residue to settle down. The original community mentioned above was centrifuged at 10,000× *g* for 10 min after 60 days to obtain the cells. The gathered cells underwent two washes with sterile acidified water (pH 2.0) followed by resuspension in 10 mL of 9K medium. Cells gathered at the initial density of inoculation were transferred into Erlenmeyer flasks, containing 100 mL sterilized 9K medium and chalcopyrite concentrate (1% pulp density). This experimental group was named D1. The mixed bacterial consortium from D1 after 60 days was added to Erlenmeyer flasks containing 100 mL sterilized 9K medium and chalcopyrite concentrate (2% pulp density). This experimental group was named D2. The procedure was repeated to collect the mixed bacterial consortium from D2 and add it to Erlenmeyer flasks containing chalcopyrite (3% pulp density). This experimental group was named D3. As a control group, the mixed bacterial consortium collected in D1 was added to Erlenmeyer flasks containing chalcopyrite (3% pulp density). This control group was named Control.

To determine cell density, pH, oxidation reduction potential (ORP), and metal ion levels, samples from both the experimental and control groups were periodically taken out of flasks. Each instance involved transferring 2 mL of the bioleaching solution into a sterile tube. The mixture underwent centrifugation at a force of 2000× *g* to let the ore residue settle down. The supernatant was withdrawn for the determination of all parameters. The pH was determined using a pHS-3E acidimeter (LEICI, Shanghai, China) and ORP (Ag/AgCl) was determined using a platinum electrode. Bacteria were counted using a CX31 light microscope (Olympus, Tokyo, Japan). Total iron (tFe) and copper ion concentrations in solution were determined using an inductively coupled plasma emission spectrophotometer (Perkin Elmer, Norwalk, CT, USA). Ferrous iron was determined using the o-phenanthroline method [32].

2.3. Characterization of Ore Residues

The original chalcopyrite sample and those of experimental and control groups after 60 days were separately collected for mineral characterization. Ore residues were withdrawn from the bioleaching solution. Subsequently, these residues were cleaned using pre-cooling ddH_2O at 4 °C with a pH of 2.0, repeated three times to eliminate any remaining solutions, and dried in a DZF-60508 vacuum drying chamber (YIHENG, Shanghai, China) at 25 °C temperature for 24 h. The corrosion of chalcopyrite was examined under a Quanta 250 ESEM (FEI, Hillsboro, OR, USA), operating at 15 kV with a secondary electron detector at a probe current between 140 and 145 pA. Components of ore residues were analyzed using XRD (Panalytical, X'pert Pro, Almelo, The Netherlands) with Cu Kα radiation (40 kV, 35 mA) conducted from 5° to 90° (2θ) at a goniometer speed of 5°/min.

2.4. Electrochemical Experiments

Original chalcopyrite and residues of experimental and control groups after 60 days were collected. All samples were pressed and prepared into carbon paste electrodes for electrochemical experiments. All experiments utilized 50 milliliters of iron-free 9K medium as the electrolyte to ensure the purity of the experimental environment. The experiments employed a three-electrode system, which included a chalcopyrite electrode serving as the working electrode with an effective working area of 1 cm^2, specifically designed for electrochemical reactions; a silver/silver chloride electrode acting as the reference electrode, providing a stable potential reference; and a graphite electrode serving as the counter electrode, together completing the electrical circuit for the electrochemical reactions. Prior to the commencement of the experiments, the chalcopyrite working electrode was carefully embedded in a specially designed electrode holder to secure its position and ensure uniform contact with the electrolyte. To achieve optimal electrochemical activity and surface smoothness, the surface of the chalcopyrite electrode was meticulously polished with a 3000-mesh emery cloth. In all tests, the same distance was maintained between the reference and working electrodes. Electrochemical measurements were performed at 6 °C using a VersaSTAT equipped with Model 273A potentiostat/galvanostat (EG&G Princeton Applied Research, Oak Ridge, TN, USA) controlled by the Power-Suite program. Cyclic Voltammetry (CV) tests were performed at a scan rate of 20 mV/s. The electrodes were immersed in electrolyte for half an hour before the experiments to maintain their condition [33]. It is essential to operate Open Circuit Potential (OCP) for 20 min to stabilize chalcopyrite electrodes before experiments. In CV, the scanning potential started from the OCP, went up to +600 mV, then reversed to −800 mV, and finally returned to OCP, at a rate of 20 mV/s. Potentiodynamic polarization curves were obtained by changing the electrode potential from −600 mV to +300 mV (vs. OCP), at a scan rate of 2 mV/s.

2.5. Sequencing of Prokaryotic 16S rRNA Gene Sequences

Bacterial communities from both experimental and control groups were individually collected into sterilized centrifuge tubes after 60 days. To dislodge the adherent cells from the minerals, a 10 min vigorous vortexing was performed with the addition of 1 g of glass beads. After vortexing, samples were subjected to centrifugation at 2500× *g* for 2 min to pellet the ore residues, leaving the supernatant for further processing. The supernatants were then centrifuged at 10,000× *g* at 4 °C for an additional 10 min to pellet the total bacterial cells. Genomic DNA was extracted following established protocols [34]. DNA integrity was verified via agarose gel electrophoresis with ethidium bromide staining. The DNA concentration was determined using a ND-1000 spectrophotometer (NanoDrop Technologies, Wilmington, DE, USA). For the 16S rRNA gene's V4 hypervariable region, amplification and sequencing protocols were as detailed in the literature [35]. In summary, PCR amplification was conducted using primers 515F and 806R [36], incorporating a label, adapter, pad, and two-base linker for library construction with the purified PCR products.

3. Results and Discussion

3.1. Bioleaching Experiments

The parameters of the experimental and control groups in the bioleaching of chalcopyrite at 6 °C are shown in Figure 1. Among the experimental groups, the lag phase of microorganisms in D1 was significantly shorter than that in the other groups, indicating that low pulp concentrations were more beneficial for microbial growth [37]. In addition, microorganisms in D1 showed the fastest growth rate during the logarithmic growth period, with their cell concentration reaching the highest cell density of 7.02×10^8 cells/mL on day 36. In contrast, the lag period of microorganisms in groups D2 and D3 was extended; they, respectively, entered the logarithmic growth period on days 12 and 15 of bioleaching, and reached their maximum concentrations on days 45 and 51, with bacterial concentrations of 6.8×10^8 cells/mL and 4.8×10^8 cells/mL, respectively. These results suggested that the maximum concentration of bacteria showed a decreasing trend as the domestication process progressed. In particular, the maximum cell density of D3 was significantly higher than that of Control (3.22×10^8 cells/mL), demonstrating that the domestication process effectively enhanced the tolerance of the low-temperature bacterial community to chalcopyrite.

As shown in Figure 1b, the pH of both the experimental and control groups presented a decreasing trend. The pH value of the experimental group started to decrease prior to the control group and the rate of decrease was significantly faster than that of the control group. This was mainly due to the generation of H^+ during the oxidation of S^{2-} to SO_4^{2-} and Fe^{2+} to Fe^{3+} [38]. The higher cell density in the experimental group enhanced the microorganisms' ability to utilize Fe^{2+}, improving the oxidation process on the chalcopyrite surface [39]. Consequently, the domestication process was likely to promote the reduction in pH.

The changes in the concentrations of Fe^{2+} and Fe^{3+} are depicted in Figure 1c. Initially, the concentration of Fe^{2+} increased and then rapidly decreased. In the later stages of bioleaching, the content of Fe^{2+} in the solution was low in all groups, with iron ions predominantly existing as Fe^{3+}. The ORP value was mainly determined by the ratio of Fe^{3+} and Fe^{2+}. In the early stages, the ratio of Fe^{3+}/Fe^{2+} was relatively low. Then, as the oxidation of Fe^{2+} by microorganisms accelerated, the concentration of Fe^{3+} gradually increased, while the concentration of Fe^{2+} decreased accordingly. This change process aligned with the trend of ORP (Figure 1d). In the control group, ORP changed slowly. This was primarily because the high pulp concentration inhibited microbial activity, thus decelerating the oxidation rate of Fe^{2+} to Fe^{3+}.

The variation in Cu^{2+} concentration is illustrated in Figure 1e,f. The bioleaching efficiency of copper ions in the experimental group always surpassed that of the control group. At the same pulp concentration, the bioleaching rate of group D3 reached 23.3% at 50 days, with a bioleaching amount of 2.19 g/L, while that of Control was 11.4%. A previous study, using a T7 mixed culture to extract chalcopyrite concentrate, found that the copper bioleaching rate merely reached 16% after 62 days [40]. The mixed bacteria enriched in the Yulong Snow Mountain could only reach the bioleaching rate of 11.2% [30]. Combined with the growth curve analysis, this might indicate that domestication improves the bioleaching rate by increasing the tolerance of the community to mineral concentration.

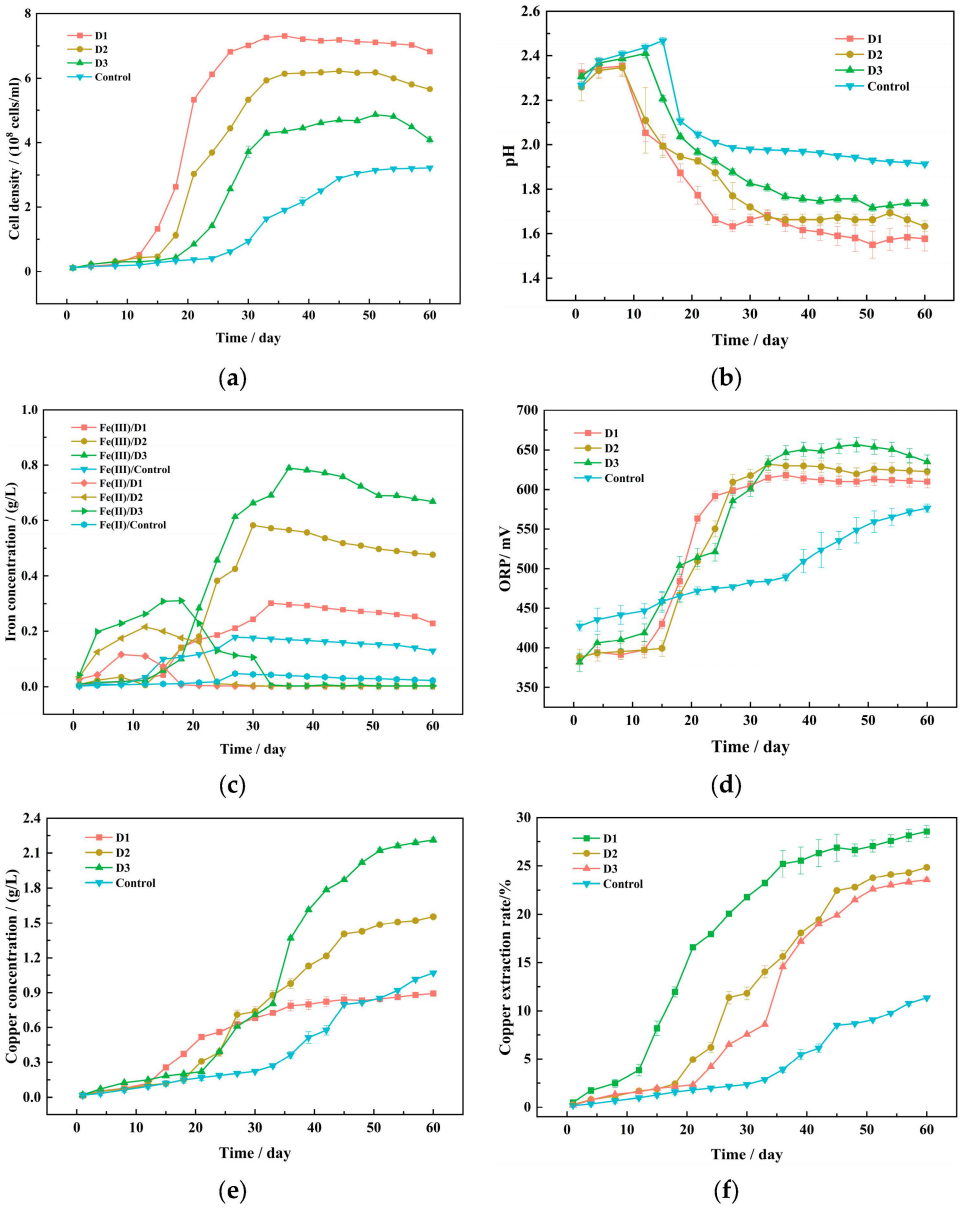


Figure 1. Changes in parameters during the bioleaching process of chalcopyrite between the experimental groups and the control group: growth curve (**a**), pH value (**b**), concentration of Fe^{3+} and Fe^{2+} (**c**), ORP (**d**), concentration of copper ions (**e**), and copper extraction rate (**f**).

3.2. Surface Morphology of Chalcopyrite

The surface morphology of the original chalcopyrite, as well as the chalcopyrite in experimental and control groups after bioleaching, were observed using SEM (Figure 2). Prior to bioleaching, the chalcopyrite surface was smooth (Figure 2a). After 60 days, the minerals of the control group produced fewer corrosion pits (Figure 2e), while those of the experimental groups had more irregular corrosion pits (Figure 2b–d). These pits might be caused by extracellular polymeric substances (EPSs) produced by microorganisms and trivalent iron ions in solution [41], which aligned with the observation that the Fe^{3+} concentration was higher in the experimental groups than in the control group. Numerous particles with indistinct edges were formed within the mineral pores of the experimental groups, while the phenomenon was less obvious in the control group. This might be due to the stronger chemotaxis of bacteria in the experimental groups compared to that in the control group [42], as well as a significantly higher density of microbial cells in the

experimental groups. These observations suggested that the corrosion degree of the ore sample after domestication was higher than that before domestication.

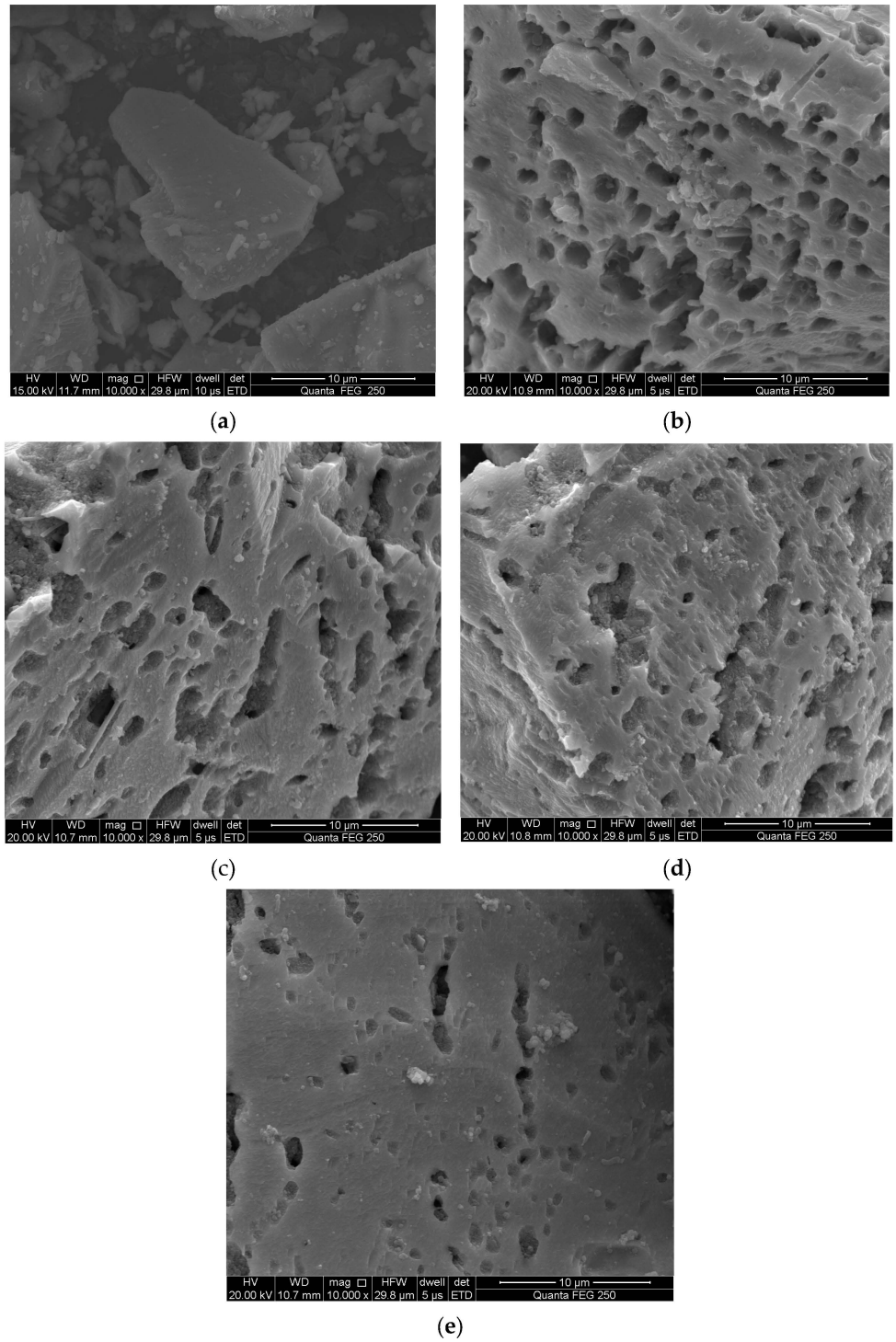


Figure 2. SEM images of original chalcopyrite surface (**a**) and leached chalcopyrite in experimental groups (**b**–**d**) and control group (**e**).

3.3. X-ray Diffraction Analysis

Passivation often occurs in the process of bioleaching, and the substances that cause passivation may be elemental sulfur (S^0), polysulfide (S_n^{2-}), or jarosite (SO_4^{2-}) [43–45]. XRD analyses were performed on the ore samples prior to bioleaching, as well as the chalcopyrite from both the experimental and control groups after bioleaching (Figure 3).

The major peak of the pre-bioleaching samples was chalcopyrite. The main peak was also chalcopyrite after bioleaching. There was no production of jarosite. Peng et al. found the same phenomenon when bioleaching chalcopyrite using *Acidithiobacillus ferrivorans* under low-temperature conditions [9]. The peak intensity of chalcopyrite in both the experimental and control groups was reduced compared with the original ore samples. The experimental groups decreased more, which might indicate that the solubility of the domesticated ore samples was higher than that before domestication.

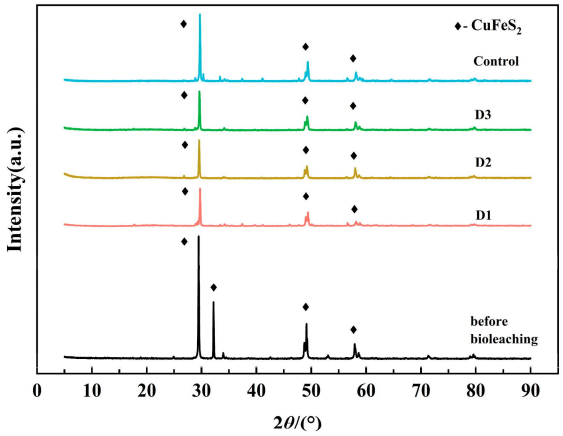


Figure 3. XRD analysis of the phase composition of original chalcopyrite and leached chalcopyrite in experimental groups and control group.

3.4. Electrochemical Analyses

3.4.1. Cyclic Voltammograms

Figure 4 depicts all cyclic voltammetry curves, which exhibited similar trends between the experimental and control groups. All curves featured one anodic peak (A1), along with two cathodic peaks (C1, C2). The A1 peak, known as the "leading peak", was a common anodic peak of chalcopyrite. The A1 peak was closely related to the electrochemical oxidation process of chalcopyrite. Chalcopyrite's dissolution was fundamentally an electrochemical phenomenon, primarily characterized by the redox interactions of its constituent elements: iron, sulfur, and copper. Owing to iron's reduced oxidation potential, it experienced preferential oxidation, subsequently being liberated into the solution. As described in Equations (1) and (2), it was attributed to the oxidation of chalcopyrite, resulting in the selective release of iron and the formation of intermediate nonstoichiometric chalcopyrite ($Cu_{1-x}Fe_{1-y}S_{2-z}$, (y > x)) and covellite (CuS) [46,47].

$$CuFeS_2 = Cu_{1-x}Fe_{1-y}S_{2-z} + xCu^{2+} + yFe^{2+} + zS^0 + 2(x + y)e^- \quad (1)$$

$$CuFeS_2 = 0.75CuS + 0.25Cu^{2+} + Fe^{2+} + 1.25S^0 + 2.5e^- \quad (2)$$

During the reverse potential scanning, a cathodic peak labeled C1 emerged at approximately 100 mV, suggesting its involvement in the reduction process of Fe^{3+}, Cu^{2+}, and S^0. A distinct reduction peak, C2, was observed at a potential of about −370 mV. This peak was closely related to the reduction process of chalcopyrite and covellite, which could be described by Equations (3) and (4) [48,49].

$$2CuS + 2H^+ + 2e^- = Cu_2S + H_2S \quad (3)$$

$$2CuFeS_2 + 6H^+ + 2e^- = Cu_2S + 2Fe^{2+} + 3H_2S \quad (4)$$

Peak C3 occurred at potentials below −500 mV. Velásquez et al. showed that this peak corresponded to the reduction reaction of covellite, referring to Equation (5) [50].

$$Cu_2S + H_2O + 2e^- = 2Cu + HS^- + OH^- \quad (5)$$

In the subsequent process of the reverse potential scanning, faint peaks A3 and A4 appeared, which were uncommon during the dissolution of chalcopyrite. A3 represented the oxidation of copper, leading to the formation of chalcocite as an intermediate product in the bioleaching process. The A4 peak corresponded to the oxidation of chalcocite, which further resulted in the production of Cu-S intermediate species that were crucial for the subsequent electrochemical reactions. These processes are detailed in Equations (6) and (7) [18].

$$2Cu + HS^- + OH^- = Cu_2S + H_2O + 2e^- \quad (6)$$

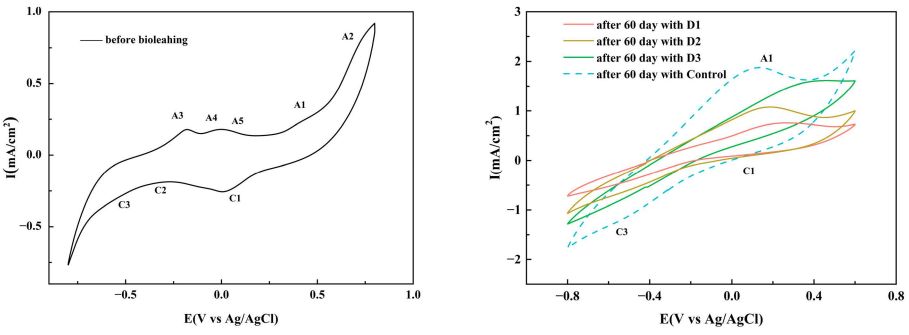
$$Cu_2S = Cu_{1.92}S + 0.08Cu^{2+} + 0.16e^- \quad (7)$$

At a more positive potential, there was another peak, A5. It has been reported that this peak may be related to the oxidation of CuxS ($1 < x < 2$) such as djurleite and geerite (Equations (8) and (9)) [49].

$$Cu_{1.92}S = Cu_{1.6}S + 0.32Cu^{2+} + 0.64e^- \quad (8)$$

$$Cu_{1.6}S = CuS + 0.60Cu^{2+} + 1.20e^- \quad (9)$$

After 60 days, the A1 peak in the control group demonstrated a significant negative shift compared to the experimental group. This suggested that the chalcopyrite in the control group was more readily converted to Cu_2S or intermediate non-stoichiometric chalcopyrite, according to Equations (1) and (2). The enhancement of current density indicated that the products exhibited good electrochemical activity, which facilitated charge transfer and rendered the reaction more facile [51]. Concurrently, the A2 peak of the control group also exhibited a notable negative shift, and the current densities of the cathodic peaks C1 and C2 surpassed those of the experimental groups, proving that the redox reactions associated with chalcopyrite dissolution were more violent in the control group. As is shown in Figure 4, characteristic peaks of chalcopyrite in the experimental groups were indistinct, and their curves appeared flat, which indicated a diminished electrochemical response, whereas the bioleaching rate in the experimental groups exceeded that of the control group, implying that the domestication process effectively enhanced bioleaching efficiency.



(**a**) (**b**)

Figure 4. Cyclic voltammograms of chalcopyrite electrodes of original chalcopyrite (**a**) and leached chalcopyrite in experimental groups and in control group (**b**).

3.4.2. Potentiodynamic Polarization

A series of potentiodynamic polarization experiments were carried out after bioleaching (Figure 5). As can be seen from Table 1, a set of electrochemical parameters were calculated from these curves, encompassing corrosion current (Icorr) and corrosion potential (Ecorr), along with the slopes associated with anodic (b_a) and cathodic (b_c) reactions. According to the Tafel formula, the expressions of b_a and b_c were as follows (Equation (10)):

$$b_a = 2.303RT/n\alpha F \qquad b_c = 2.303RT/n\beta F \quad (10)$$

The E_{corr} value of D3 was higher than that of Control, while the I_{corr} value was lower than that of Control. This result was in agreement with the results of the slope of the end-point bioleaching rate (Figure 1e). The study found that E_{corr} in Control (184 mV) was lower than that of the D3 group (196.9 mV), indicating that the corrosion tendency of chalcopyrite was greater in Control. In addition, the I_{corr} of Control (12.99 μA/cm^2) was higher than that of D3 (11.01 μA/cm^2), which indicated that the corrosion rate was faster. The increase in E_{corr} indicated that chalcopyrite surface was covered by the products during bioleaching [52], which was unfavorable to its oxidation reaction. The reduction in I_{corr} suggested that these products inhibited the reaction rate. It further confirmed that the rates of oxidation reaction and electron transfer were higher in Control.

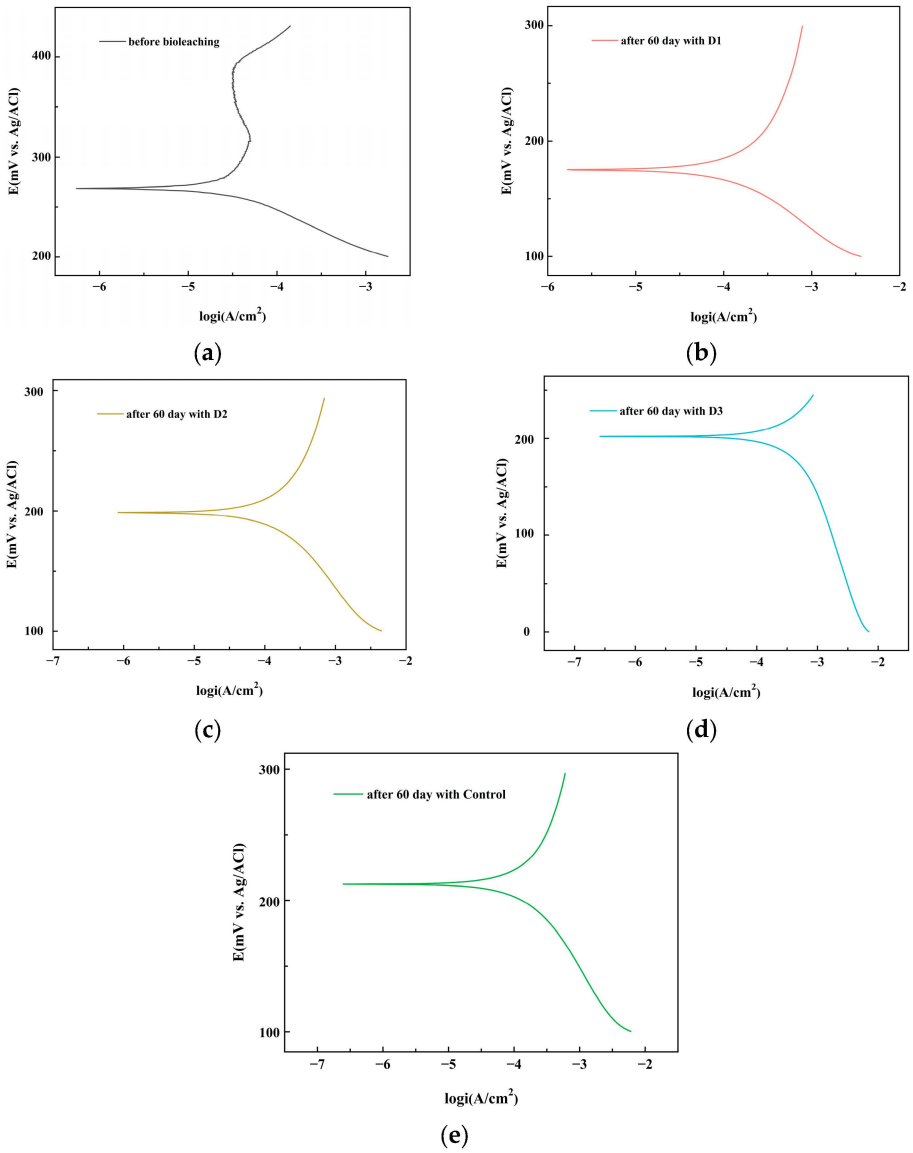


Figure 5. Potentiodynamic polarization curve of chalcopyrite electrodes of original chalcopyrite (**a**) and leached chalcopyrite in experimental groups (**b**–**d**) and in control group (**e**).

The b_a and b_c of the chalcopyrite electrodes in the experimental groups were higher than those of the control group (Table 2). b_a and b_c are usually correlated with the Tafel slope, and their larger values could imply that the reaction rate was faster. It was found that the charge transfer coefficients (β and α) were increased, which implied that domestication was beneficial to the exchange and transfer of the electron of the electrode reactions, thus promoting the oxidation and decomposition of chalcopyrite. This suggested that

domestication might alter the electrochemical properties of the chalcopyrite surface in some way, accelerating the mineral's oxidative breakdown.

Table 1. Domestication experiment.

System	Name	Pulp Density	Microbial Consortium
Experimental groups	D1	1%	original community
	D2	2%	D1
	D3	3%	D2
Control group	Control	3%	original community

Table 2. Polarization kinetic parameters of chalcopyrite electrodes of original chalcopyrite and leached chalcopyrite in experimental and control groups.

System	E_{corr}/mV	I_{corr}/((uA/cm^2)	b_a/(mV/decade)	b_c/(mV/decade)
Before bioleaching	260	3.79	213.6	234.6
D1	184	9.83	211.9	233.4
D2	196.9	10.58	210.8	208.9
D3	202	11.01	199.1	205
Control	218.8	12.99	179.3	150.6

3.5. Microbial Community Analysis

3.5.1. Alpha-Diversity

Compared with Control, the Shannon index showed an increasing trend and the Simpson index showed a decreasing trend in the experimental groups (Figure 6). The Shannon index of D3 was higher than that of Control and the Simpson index was lower than that of Control, indicating that the species richness and diversity of this experimental group was higher than that of Control. Combined with the previous data, the bioleaching rate and acidity of D3 were higher than those of Control, which could be attributed to the fact that the high-diversity community was more adapted to the environment [53], while acidity and soluble metal concentration were the key factors controlling the structure of the bacterial community [54].

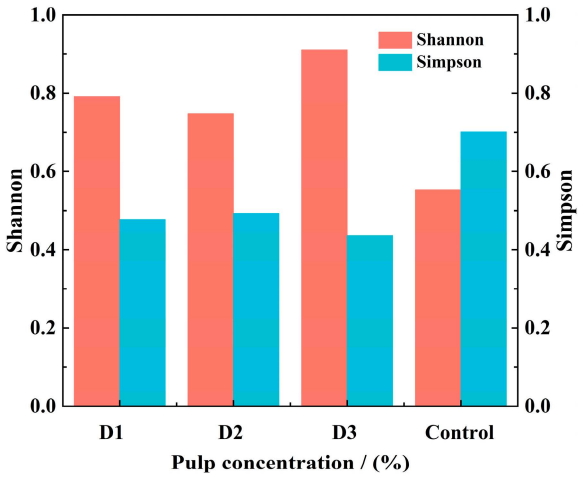


Figure 6. α-analysis in experimental and control groups after bioleaching.

3.5.2. Microbial Community Structure

The microbial community was monitored using the high-throughput sequencing of the 16S rRNA gene. All samples were collected from the experimental and control communities (Figure 7). Chord diagram was a visualization tool for biodiversity. Figure 7a showed the relationships between experimental and control group samples and microbial phyla,

while Figure 7b delineates the connections between these samples and microbial genera. In these diagrams, samples are positioned on the left side, with microbial taxonomic units (phyla or genera) listed on the right. The thickness of the chords signifies the relative abundance or significance of the corresponding taxonomic groups within the samples. A total of 58,882 high-quality sequences were obtained after 60 days. Based on the sequencing read lengths and number of OTUs, the dilution curves for all samples reached the plateau region, indicating that the sequencing depth was suitable for estimating microbial diversity.

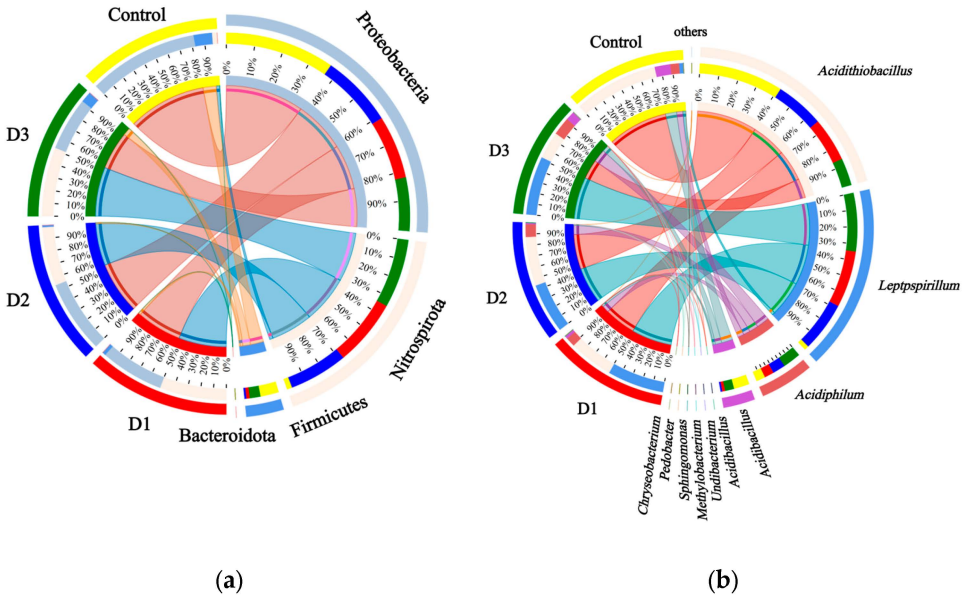


Figure 7. Analysis of species composition in experimental and control groups after bioleaching.

At the phylum level, Proteobacteria and Nitrospirota were the dominant lineages, which accounted for 86.1%–97.4% of the total biomass, followed by Firmicutes (2.04%–13.8%). The remaining phylum was Bacteroidota, but it was at an extremely low level (<1%). Down to the genus level, 18, 13, 13 and 12 OTUs were, respectively, detected in D1, D2, D3, and Control. Nine OTUs were shared by all samples. The top three dominant genera in the experimental groups were *Acidithiobacillus* spp., *Leptospirillum* spp., and *Acidiphilium* spp., cumulatively exceeding 90% of the microbial communities. This might be because all of them are acidophilic microorganisms, with strong adaptability in acidic environments. They can grow and reproduce at lower pH values, and when metabolized they produce substances such as organic acids. At the same time, these three microorganisms have the ability to oxidize and decompose minerals, thereby increasing the bioleaching rate [55–57]. *Acidithiobacillus* spp., *Acidiphilium* spp., and *Acidibacillus* spp. were the top three dominant genera in the control group. It could be seen that *Acidithiobacillus* spp. had the highest relative abundance in the experimental and control groups, which might be due to the ability of *Acidithiobacillus* spp. to survive and reproduce at low temperatures [58]. Compared to Control, the proportion of *Leptospirillum* spp. was higher in the experimental groups. This might be because high pulp concentration inhibited the survival of *Leptospirillum* spp., and *Leptospirillum* spp. was a key factor promoting biofilm formation [59]. Additionally, domestication might promote the production of diffusive signaling factors, protecting its ecological niche and enhancing the biological community's adaptability to high pulp concentration [60]. The proportions of *Acidiphilium* spp. and *Acidibacillus* spp. in D1 and D2 were quite low, while those in D3 and Control were significantly higher. This might be because *Acidiphilium* spp. and *Acidibacillus* spp. can tolerate greater shear force, thus better adapting to survive in minerals with high pulp concentration [61].

3.5.3. Comparison of Microbial Community Structures

The similarities and differences of the community structure between experimental and control groups were evaluated using principal coordinate analysis (PCoA). PCA based on OTU data delineated the β-diversity within the microbial communities, with PCA1 accounting for 91.81% of the variance in community structure, indicating its predominant role in reflecting the primary sources of community variation (Figure 8). The secondary component, PCA2, elucidated an additional 7.15% of the variance, offering supplementary insights into the community's diversity. All samples were dispersed in three quadrants. D1 and D2 were located in the same quadrant, while D3 and the control group were located in the other two quadrants. This implied that the communities of D1 and D2 had similarities, while the communities of D3 and Control had differences. this revealed that domestication induced significant changes in the community structure of the experimental and control groups. This might be due to the increase in the concentration of the pulp and the change in the mineral composition during domestication, which induced a change in the effective surface area of the minerals and a different community structure [62,63].

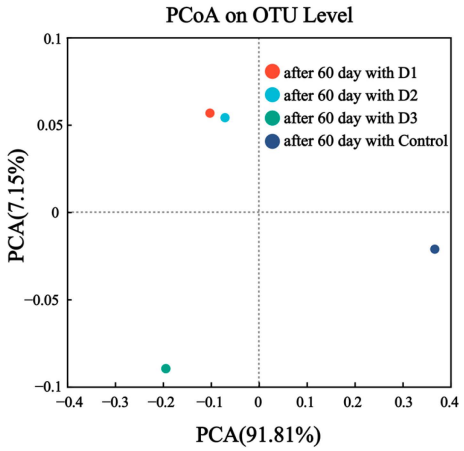


Figure 8. β-analysis in experimental and control groups after bioleaching.

4. Conclusions

The microbial community was domesticated using the method of gradually increasing pulp concentration at 6 °C. The experimental results showed that the efficiency of the bioleaching of chalcopyrite was improved after domestication. *Acidithiobacillus* spp., *Leptospirillum* spp., and *Acidiphilium* spp. were dominant in the domesticated community. Compared with Control, domestication intensified the dissolution reaction, exacerbated the corrosion of the chalcopyrite surface, and reduced the formation of passive substances. The analysis of the microbial community revealed that domestication changed the microbial structure and enhanced the adaptability of the microbial community to pulp concentration and acidic conditions. This study not only confirmed that domestication could effectively enhance bioleaching efficiency, but also revealed the mechanism behind it. This discovery has important theoretical and practical significance for improving the metal recovery efficiency in alpine mining areas and promoting the further development of low-temperature bioleaching technology.

Author Contributions: Conceptualization, W.Z. and X.J.; methodology, W.Z. and X.J.; validation, M.M. and X.J.; formal analysis, M.M. and X.J.; investigation, M.M. and X.J.; resources, W.Z.; data curation, X.J.; writing—original draft preparation, W.Z. and X.J.; writing—review and editing, X.J.; visualization, M.M. and X.J.; supervision, W.Z.; project administration, W.Z.; funding acquisition, W.Z. All authors have read and agreed to the published version of the manuscript.

Funding: This work was supported by the National Key Research and Development Program of China (No. 2019YFC1803604), the National Natural Science Foundation of China (No. 51934009, No. 52074353), the Science and Technology Project of Hunan Province (No. 2021NK1040), the Natural Science Foundation of Hunan Province (No. 2021JJ30855, No. 2021JJ30836), and the Open Foundation of the State Key Laboratory of Comprehensive Utilization of Low-Grade Refractory Gold Ores.

Data Availability Statement: Data are contained within the article.

Acknowledgments: Thanks to the reviewers for their careful suggestions and to the academic editors for their sincere affirmations. Thanks to all those who helped with the field sampling and experiments.

Conflicts of Interest: The authors declare no conflicts of interest. The funders had no role in the design of the study; in the collection, analyses, or interpretation of data; in the writing of the manuscript, or in the decision to publish the results.

References

1. Zhao, H.; Zhang, Y.; Zhang, X.; Qian, L.; Sun, M.; Yang, Y.; Zhang, Y.; Wang, J.; Kim, H.; Qiu, G. The dissolution and passivation mechanism of chalcopyrite in bioleaching: An overview. *Miner. Eng.* **2019**, *136*, 140–154. [CrossRef]
2. Panda, S.; Akcil, A.; Pradhan, N.; Deveci, H. Current scenario of chalcopyrite bioleaching: A review on the recent advances to its heap-leach technology. *Bioresour. Technol.* **2015**, *196*, 694–706. [CrossRef]
3. Xue, Z.; Feng, Y.; Li, H.; Zhu, Z.; Xu, C.; Ju, J.; Yang, Y. A comprehensive review on progresses of coal and minerals bioflotation in presence of microorganisms. *J. Environ. Chem. Eng.* **2023**, *11*, 111182. [CrossRef]
4. Ahonen, L.; Tuovinen, O.H. Temperature effects on bacterial leaching of sulfide minerals in shake flask experiments. *Appl. Environ. Microbiol.* **1991**, *57*, 138–145. [CrossRef] [PubMed]
5. Elberling, B.; Schippers, A.; Sand, W. Bacterial and chemical oxidation of pyritic mine tailings at low temperatures. *J. Contam. Hydrol.* **2000**, *41*, 225–238. [CrossRef]
6. Escobar, B.; Buccicardi, S.; Morales, G.; Wiertz, J. Biooxidation of ferrous iron and sulphide at low temperatures: Implications on acid mine drainage and bioleaching of sulphide minerals. *Hydrometallurgy* **2010**, *104*, 454–458. [CrossRef]
7. Langdahl, B.R.; Ingvorsen, K. Temperature characteristics of bacterial iron solubilisation and 14C assimilation in naturally exposed sulfide ore material at Citronen Fjord, North Greenland (83 N). *FEMS Microbiol. Ecol.* **1997**, *23*, 275–283. [CrossRef]
8. Dopson, M.; Halinen, A.K.; Rahunen, N.; Özkaya, B.; Sahinkaya, E.; Kaksonen, A.H.; Lindström, E.B.; Puhakka, J.A. Mineral and iron oxidation at low temperatures by pure and mixed cultures of acidophilic microorganisms. *Biotechnol. Bioeng.* **2007**, *97*, 1205–1215. [CrossRef]
9. Peng, T.; Chen, L.; Wang, J.; Miao, J.; Shen, L.; Yu, R.; Gu, G.; Qiu, G.; Zeng, W. Dissolution and passivation of chalcopyrite during bioleaching by *Acidithiobacillus ferrivorans* at low temperature. *Minerals* **2019**, *9*, 332. [CrossRef]
10. Li, L.; King, A.; Davis, K.; Yu, B. Electrochemical Kinetics Study of Ultrasound-Assisted Chalcopyrite Oxidation. *J. Sustain. Metall.* **2023**, *9*, 678–687. [CrossRef]
11. Zhao, C.; Yang, B.; Liao, R.; Hong, M.; Yu, S.; Liu, S.; Wang, J.; Qiu, G. Combined effect and mechanism of visible light and Ag^+ on chalcopyrite bioleaching. *Miner. Eng.* **2022**, *175*, 107283. [CrossRef]
12. Pan, H.D.; Yang, H.Y.; Tong, L.L.; Zhong, C.B.; Zhao, Y.S. Control method of chalcopyrite passivation in bioleaching. *Trans. Nonferrous Met. Soc. China* **2012**, *22*, 2255–2260. [CrossRef]
13. Gericke, M.; Pinches, A. Bioleaching of copper sulphide concentrate using extreme thermophilic bacteria. *Miner. Eng.* **1999**, *12*, 893–904. [CrossRef]
14. Gericke, M.; Pinches, A.; van Rooyen, J.V. Bioleaching of a chalcopyrite concentrate using an extremely thermophilic culture. *Int. J. Miner. Process.* **2001**, *62*, 243–255. [CrossRef]
15. Zhang, L.; Zhou, W.; Liu, Y.; Jia, H.; Zhou, J.; Wei, P.; Zhou, H. Bioleaching of dewatered electroplating sludge for the extraction of base metals using an adapted microbial consortium: Process optimization and kinetics. *Hydrometallurgy* **2020**, *191*, 105227. [CrossRef]
16. Zeng, W.; Qiu, G.; Zhou, H.; Chen, M. Electrochemical behaviour of massive chalcopyrite electrodes bioleached by moderately thermophilic microorganisms at 48 °C. *Hydrometallurgy* **2011**, *105*, 259–263. [CrossRef]
17. Zhao, H.B.; Hu, M.H.; Li, Y.N.; Zhu, S.; Qin, W.Q.; Qiu, G.Z.; Wang, J. Comparison of electrochemical dissolution of chalcopyrite and bornite in acid culture medium. *Trans. Nonferrous Met. Soc. China* **2015**, *25*, 303–313. [CrossRef]
18. Zeng, W.; Qiu, G.; Chen, M. Investigation of Cu-S intermediate species during electrochemical dissolution and bioleaching of chalcopyrite concentrate. *Hydrometallurgy* **2013**, *134*, 158–165. [CrossRef]
19. Peng, T.; Liao, W.; Wang, J.; Miao, J.; Peng, Y.; Gu, G.; Wu, X.; Qiu, G.; Zeng, W. Bioleaching and Electrochemical Behavior of Chalcopyrite by a Mixed Culture at Low Temperature. *Front. Microbiol.* **2021**, *12*, 663757. [CrossRef]
20. Akcil, A.; Ciftci, H.; Deveci, H. Role and contribution of pure and mixed cultures of mesophiles in bioleaching of a pyritic chalcopyrite concentrate. *Miner. Eng.* **2007**, *20*, 310–318. [CrossRef]
21. Gu, G.H.; Hu, K.T.; Li, S.K. Bioleaching and electrochemical properties of chalcopyrite by pure and mixed culture *of Leptospirillum ferriphilum* and *Acidthiobacillus thiooxidans*. *J. Cent. South Univ.* **2013**, *20*, 178–183. [CrossRef]

22. Zhang, Y.S.; Qin, W.Q.; Wang, J.; Zhen, S.J.; Yang, C.R.; Zhang, J.W.; Nai, S.-s.; Qiu, G.-z. Bioleaching of chalcopyrite by pure and mixed culture. *Trans. Nonferrous Met. Soc. China* **2008**, *18*, 1491–1496. [CrossRef]
23. Fomchenko, N.V.; Muravyov, M.I. Two-step biohydrometallurgical technology of copper-zinc concentrate processing as an opportunity to reduce negative impacts on the environment. *J. Environ. Manag.* **2018**, *226*, 270–277. [CrossRef]
24. Lukhele, T.; Selvarajan, R.; Nyoni, H.; Mamba, B.B.; Msagati, T.A.M. Diversity and functional profile of bacterial communities at Lancaster acid mine drainage dam, South Africa as revealed by 16S rRNA gene high-throughput sequencing analysis. *Extremophiles* **2019**, *23*, 719–734. [CrossRef]
25. Romo, E.; Weinacker, D.F.; Zepeda, A.B.; Figueroa, C.A.; Chavez-Crooker, P.; Farias, J.G. Bacterial consortium for copper extraction from sulphide ore consisting mainly of chalcopyrite. *Braz. J. Microbiol.* **2013**, *44*, 523–528. [CrossRef]
26. Latorre, M.; Paz Cortes, M.; Travisany, D.; Di Genova, A.; Budinich, M.; Reyes-Jara, A.; Hoedar, C.; Gonzalez, M.; Parada, P.; Bobadilla-Fazzini, R.A.; et al. The bioleaching potential of a bacterial consortium. *Bioresour. Technol.* **2016**, *218*, 659–666. [CrossRef]
27. Rios, D.; Bellenberg, S.; Christel, S.; Lindblom, P.; Giroux, T.; Dopson, M. Potential of single and designed mixed cultures to enhance the bioleaching of chalcopyrite by oxidation-reduction potential control. *Hydrometallurgy* **2024**, *224*, 106245. [CrossRef]
28. Halinen, A.K.; Rahunen, N.; Kaksonen, A.H.; Puhakka, J.A. Heap bioleaching of a complex sulfide ore: Part II. Effect of temperature on base metal extraction and bacterial compositions. *Hydrometallurgy* **2009**, *98*, 101–107. [CrossRef]
29. Zepeda, V.; Galleguillos, F.; Castillo, D.; Lastra, M.; Demergasso, C. Bacterial activity at low temperature in cultures derived from a low-grade copper sulphide bioleaching heap at the Escondida Mine, Chile. *Adv. Mater. Res.* **2007**, *20*, 543–546. [CrossRef]
30. Liljeqvist, M.; Rzhepishevska, O.I.; Dopson, M. Gene identification and substrate regulation provide insights into sulfur accumulation during bioleaching with the psychrotolerant acidophile *Acidithiobacillus ferrivorans*. *Appl. Environ. Microbiol.* **2013**, *79*, 951–957. [CrossRef]
31. Johnson, D.B.; Rolfe, S.; Hallberg, K.B.; Iversen, E. Isolation and phylogenetic characterization of acidophilic microorganisms indigenous to acidic drainage waters at an abandoned Norwegian copper mine. *Environ. Microbiol.* **2001**, *3*, 630–637. [CrossRef] [PubMed]
32. Tamura, H.; Goto, K.; Yotsuyanagi, T.; Nagayama, M. Spectrophotometric determination of iron (II) with 1, 10-phenanthroline in the presence of large amounts of iron (III). *Talanta* **1974**, *21*, 314–318. [CrossRef] [PubMed]
33. Ghahremaninezhad, A.; Dixon, D.; Asselin, E. Electrochemical and XPS analysis of chalcopyrite ($CuFeS_2$) dissolution in sulfuric acid solution. *Electrochim. Acta* **2013**, *87*, 97–112. [CrossRef]
34. Wu, X.; Wu, X.; Shen, L.; Li, J.; Yu, R.; Liu, Y.; Qiu, G.; Zeng, W. Whole genome sequencing and comparative genomics analyses of *Pandoraea* sp. XY-2, a new species capable of biodegrade tetracycline. *Front. Microbiol.* **2019**, *10*, 33. [CrossRef] [PubMed]
35. Xiao, Y.; Xu, Y.; Dong, W.; Liang, Y.; Fan, F.; Zhang, X.; Zhang, X.; Niu, J.; Ma, L.; She, S. The complicated substrates enhance the microbial diversity and zinc leaching efficiency in sphalerite bioleaching system. *Appl. Microbiol. Biotechnol.* **2015**, *99*, 10311–10322. [CrossRef]
36. Rinke, C.; Lee, J.; Nath, N.; Goudeau, D.; Thompson, B.; Poulton, N.; Dmitrieff, E.; Malmstrom, R.; Stepanauskas, R.; Woyke, T. Obtaining genomes from uncultivated environmental microorganisms using FACS-based single-cell genomics. *Nat. Protoc.* **2014**, *9*, 1038–1048. [CrossRef]
37. Wang, Y.; Zeng, W.; Qiu, G.; Chen, X.; Zhou, H. A Moderately Thermophilic Mixed Microbial Culture for Bioleaching of Chalcopyrite Concentrate at High Pulp Density. *Appl. Environ. Microbiol.* **2014**, *80*, 741–750. [CrossRef] [PubMed]
38. Nguyen, K.A.; Borja, D.; You, J.; Hong, G.; Jung, H.; Kim, H. Chalcopyrite Bioleaching Using Adapted Mesophilic Microorganisms: Effects of Temperature, Pulp Density, and Initial Ferrous Concentrations. *Mater. Trans.* **2018**, *59*, 1860–1866. [CrossRef]
39. Rohwerder, T.; Gehrke, T.; Kinzler, K.; Sand, W. Bioleaching review part A: Progress in bioleaching: Fundamentals and mechanisms of bacterial metal sulfide oxidation. *Appl. Microbiol. Biotechnol.* **2003**, *63*, 239–248. [CrossRef]
40. Kocaman, A.T.; Cemek, M.; Edwards, K.J. Kinetics of pyrite, pyrrhotite, and chalcopyrite dissolution by *Acidithiobacillus ferrooxidans*. *Can. J. Microbiol.* **2016**, *62*, 629–642. [CrossRef]
41. Zhang, R.; Bellenberg, S.; Castro, L.; Neu, T.R.; Sand, W.; Vera, M. Colonization and biofilm formation of the extremely acidophilic archaeon *Ferroplasma acidiphilum*. *Hydrometallurgy* **2014**, *150*, 245–252. [CrossRef]
42. Sand, W.; Gehrke, T. Extracellular polymeric substances mediate bioleaching/biocorrosion via interfacial processes involving iron(III) ions and acidophilic bacteria. *Res. Microbiol.* **2006**, *157*, 49–56. [CrossRef]
43. Yang, Y.; Liu, W.; Chen, M. A copper and iron K-edge XANES study on chalcopyrite leached by mesophiles and moderate thermophiles. *Miner. Eng.* **2013**, *48*, 31–35. [CrossRef]
44. Klauber, C.; Parker, A.; van Bronswijk, W.; Watling, H. Sulphur speciation of leached chalcopyrite surfaces as determined by X-ray photoelectron spectroscopy. *Int. J. Miner. Process.* **2001**, *62*, 65–94. [CrossRef]
45. Zhu, W.; Xia, J.L.; Yang, Y.; Nie, Z.Y.; Zheng, L.; Ma, C.Y.; Zhang, R.Y.; Peng, A.A.; Tang, L.; Qiu, G.Z. Sulfur oxidation activities of pure and mixed thermophiles and sulfur speciation in bioleaching of chalcopyrite. *Bioresour. Technol.* **2011**, *102*, 3877–3882. [CrossRef]
46. Nicol, M.J. The electrochemistry of chalcopyrite in alkaline solutions. *Hydrometallurgy* **2019**, *187*, 134–140. [CrossRef]
47. Gu, G.; Hu, K.; Zhang, X.; Xiong, X.; Yang, H. The stepwise dissolution of chalcopyrite bioleached by *Leptospirillum ferriphilum*. *Electrochim. Acta* **2013**, *103*, 50–57. [CrossRef]
48. Biegler, T.; Horne, M. The electrochemistry of surface oxidation of chalcopyrite. *J. Electrochem. Soc.* **1985**, *132*, 1363. [CrossRef]

49. Arce, E.A.; González, I. A comparative study of electrochemical behavior of chalcopyrite, chalcocite and bornite in sulfuric acid solution. *Int. J. Miner. Process.* **2002**, *67*, 17–28. [CrossRef]
50. Velásquez, P.; Leinen, D.; Pascual, J.; Ramos-Barrado, J.R.; Cordova, R.; Gómez, H.; Schrebler, R. XPS, SEM, EDX and EIS study of an electrochemically modified electrode surface of natural chalcocite (Cu_2S). *J. Electroanal. Chem.* **2001**, *510*, 20–28. [CrossRef]
51. Zhao, H.; Huang, X.; Wang, J.; Li, Y.; Liao, R.; Wang, X.; Qiu, X.; Xiong, Y.; Qin, W.; Qiu, G. Comparison of bioleaching and dissolution process of p-type and n-type chalcopyrite. *Miner. Eng.* **2017**, *109*, 153–161. [CrossRef]
52. O'Connor, G.; Lepkova, K.; Eksteen, J.; Oraby, E. Electrochemical behaviour of copper in alkaline glycine solutions. *Hydrometallurgy* **2018**, *181*, 221–229. [CrossRef]
53. Tao, J.; Liu, X.; Luo, X.; Teng, T.; Jiang, C.; Drewniak, L.; Yang, Z.; Yin, H. An integrated insight into bioleaching performance of chalcopyrite mediated by microbial factors: Functional types and biodiversity. *Bioresour. Technol.* **2021**, *319*, 124219. [CrossRef]
54. Yang, Y.; Shi, W.; Wan, M.; Zhang, Y.; Zou, L.; Huang, J.; Qiu, G.; Liu, X. Diversity of bacterial communities in acid mine drainage from the Shen-bu copper mine, Gansu province, China. *Electron. J. Biotechnol.* **2008**, *11*, 1–12. [CrossRef]
55. Tavakoli, H.Z.; Abdollahy, M.; Ahmadi, S.J.; Darban, A.K. Kinetics of uranium bioleaching in stirred and column reactors. *Miner. Eng.* **2017**, *111*, 36–46. [CrossRef]
56. Wang, X.; Liao, R.; Zhao, H.; Hong, M.; Huang, X.; Peng, H.; Wen, W.; Qin, W.; Qiu, G.; Huang, C.; et al. Synergetic effect of pyrite on strengthening bornite bioleaching by *Leptospirillum ferriphilum*. *Hydrometallurgy* **2018**, *176*, 9–16. [CrossRef]
57. Huo, X.; Liu, J.; Hong, X.; Bai, H.; Chen, Z.; Che, J.; Yang, H.; Tong, Y.; Feng, S. Enhancing column bioleaching of chalcocite by isolated iron metabolism partners *Leptospirillum ferriphilum*/*Acidiphilium* sp. coupling with systematically utilizing cellulosic waste. *Bioresour. Technol.* **2024**, *394*, 130193. [CrossRef]
58. Ccorahua-Santo, R.; Eca, A.; Abanto, M.; Guerra, G.; Ramirez, P. Physiological and comparative genomic analysis of *Acidithiobacillus ferrivorans* PQ33 provides psychrotolerant fitness evidence for oxidation at low temperature. *Res. Microbiol.* **2017**, *168*, 482–492. [CrossRef]
59. Bellenberg, S.; Salas, B.; Ganji, S.; Jorquera-Roman, C.; Valenzuela, M.L.; Buetti-Dinh, A.; Unelius, C.R.; Dopson, M.; Vera, M. Diffusible signal factor signaling controls bioleaching activity and niche protection in the acidophilic, mineral-oxidizing leptospirilli. *Sci. Rep.* **2021**, *11*, 16275. [CrossRef]
60. Rodríguez, Y.; Ballester, A.; Blázquez, M.L.; González, F.; Muñoz, J.A. Study of bacterial attachment during the bioleaching of pyrite, chalcopyrite, and sphalerite. *Geomicrobiol. J.* **2003**, *20*, 131–141. [CrossRef]
61. Liu, Y.; Wang, J.; Hou, H.; Chen, G.; Liu, H.; Liu, X.; Shen, L. Effect of Introduction of Exogenous Strain *Acidithiobacillus thiooxidans* A01 on Structure and Function of Adsorbed and Planktonic Microbial Consortia during Bioleaching of Low-Grade Copper Sulfide. *Front. Microbiol.* **2020**, *10*, 3034. [CrossRef] [PubMed]
62. Valencia, P.; Acevedo, F. Are bioleaching rates determined by the available particle surface area concentration? *World J. Microbiol. Biotechnol.* **2009**, *25*, 101–106. [CrossRef]
63. Wang, X.; Ma, L.; Wu, J.; Xiao, Y.; Tao, J.; Liu, X. Effective bioleaching of low-grade copper ores: Insights from microbial cross. *Bioresour. Technol.* **2020**, *308*, 123273. [CrossRef] [PubMed]

Disclaimer/Publisher's Note: The statements, opinions and data contained in all publications are solely those of the individual author(s) and contributor(s) and not of MDPI and/or the editor(s). MDPI and/or the editor(s) disclaim responsibility for any injury to people or property resulting from any ideas, methods, instructions or products referred to in the content.